Cell-autonomous repression of shh by transcription factor pax6 regulates diencephalic patterning by controlling the central diencephalic organizer

Cell Reports
Article

Cell-Autonomous Repression of *Shh* by Transcription Factor Pax6 Regulates Diencephalic Patterning by Controlling the Central Diencephalic Organizer

Isabel Martín Caballero,[1,3] Martine N. Manuel,[1,3] Michael Molinek,[1] Idoia Quintana-Urzainqui,[1] Da Mi,[1] Tomomi Shimogori,[2] and David J. Price[1,*]
[1]Centre for Integrative Physiology, University of Edinburgh, Edinburgh EH8 9XD, UK
[2]RIKEN Brain Science Institute, Saitama 351-0198, Japan
[3]Co-first author
*Correspondence: david.price@ed.ac.uk
http://dx.doi.org/10.1016/j.celrep.2014.07.051

SUMMARY

During development, region-specific patterns of regulatory gene expression are controlled by signaling centers that release morphogens providing positional information to surrounding cells. Regulation of signaling centers themselves is therefore critical. The size and the influence of a Shh-producing forebrain organizer, the zona limitans intrathalamica (ZLI), are limited by Pax6. By studying mouse chimeras, we find that Pax6 acts cell autonomously to block *Shh* expression in cells around the ZLI. Immunoprecipitation and luciferase assays indicate that Pax6 can bind the *Shh* promoter and repress its function. An analysis of chimeras suggests that many of the regional gene expression pattern defects that occur in *Pax6*$^{-/-}$ diencephalic cells result from a non-cell-autonomous position-dependent defect of local intercellular signaling. Blocking Shh signaling in *Pax6*$^{-/-}$ mutants reverses major diencephalic patterning defects. We conclude that Pax6's cell-autonomous repression of *Shh* expression around the ZLI is critical for many aspects of normal diencephalic patterning.

INTRODUCTION

Our understanding of the mechanisms that regulate the organization of developing tissues is based on the idea that cells gain information determining their fates by monitoring the levels of morphogens released by discrete signaling centers, or organizers, in their vicinity (Rogers and Schier, 2011). Much less is known about the mechanisms that regulate the organizers. One possibility is that feedback from transcription factors whose expression is regulated by morphogens contributes to the control of the organizers and their morphogen production. The identification of such mechanisms is particularly interesting because they are likely to play a major role in enhancing the precision, stability, and robustness of gene expression patterns in the developing embryo (Sokolowski et al., 2012). Here, we tested whether feedback via the transcription factor Pax6 regulates the size and function of a forebrain organizer, the zona limitans intrathalamica (ZLI).

The diencephalon is the caudalmost component of the forebrain and contains the thalamus. During development, interactions between genes expressed around and within the thalamic anlage establish regions with different identities and fates along the embryonic rostral-caudal axis. The transcription factors Fezf1 and Fezf2 specify a rostral diencephalic domain (the future prethalamus; Hirata et al., 2006; Jeong et al., 2007), whereas the transcription factors Otx2 and Irx1 specify a caudal diencephalic domain (the future thalamus; Hirata et al., 2006). The ZLI forms as a thin strip of tissue in the progenitor cell layer at the interface between these domains. It contributes to the organization of the regions around it mainly through its expression of the diffusible morphogen Shh (Hashimoto-Torii et al., 2003; Jeong et al., 2011; Kiecker and Lumsden, 2004; Scholpp et al., 2006; Scholpp and Lumsden, 2010; Zhou et al., 2004; Robertshaw et al., 2013).

The ZLI forms at around embryonic days 9–10 (E9–E10) in the mouse. It appears as a thin spike of Shh-expressing tissue extending from basal plate through alar plate toward roof plate (Shimamura et al., 1995). Immediately caudal to it, a small rostral area (called pTh-R; Figure 1B), which comprises thalamic progenitors exposed to relatively high levels of Shh, expresses *Ascl1* and *Nkx2.2* and generates mostly GABAergic neurons that contribute to the ventral lateral geniculate (vLG) nucleus (Inamura et al., 2011; Suzuki-Hirano et al., 2011; Vue et al., 2007; Robertshaw et al., 2013). A larger region of thalamic progenitors caudal to pTh-R, called pTh-C (Figure 1B), expresses *Ngn2* and *Olig3* rather than *Ascl1* and *Nkx2.2* and generates glutamatergic neurons that innervate cortex (Vue et al., 2007; Robertshaw et al., 2013).

Forebrain expression of *Pax6* is dynamic. It starts in the neural plate and is initially throughout the entire alar forebrain neuroepithelium (Mastick et al., 1997). From around E9–E10, Pax6 is repressed in the ZLI by developing Shh expression (Ericson et al., 1997; Macdonald et al., 1995; Robertshaw et al., 2013). Pax6 is retained by prethalamic progenitors and postmitotic cells and by thalamic progenitors; the latter express it in a gradient, with Pax6 levels increasing with distance from the ZLI. Mutant mice lacking Pax6 show progressive defects of diencephalic

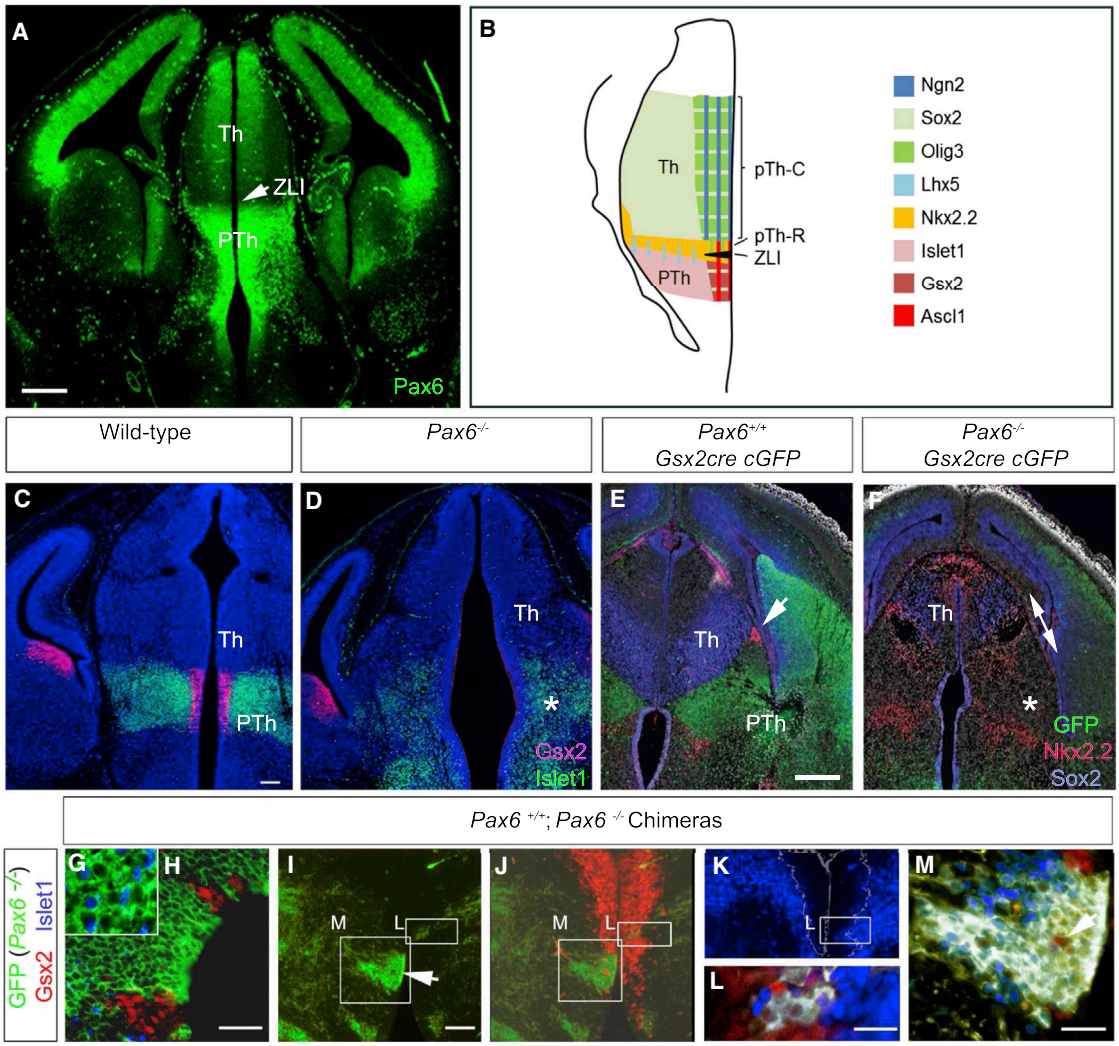

Figure 1. Cells of the Prethalamus Require Pax6 Cell Autonomously for *Gsx2* Expression

(A) Pax6 expression at E12.5. Th, thalamus; PTh, prethalamus.

(B) Normal expression patterns of genes studied here. Expression in the ZLI is examined later.

(C and D) Gsx2 and Islet1 expression at E13.5. Asterisk in (D) points to the position of prethalamus.

(E and F) Expression of Sox2, Nkx2.2, and a conditional GFP reporter (*cGFP*) in E15.5 embryos carrying a *Gsx2cre* transgene. Arrow in (E) points to the vLG. Double arrow in (F) points to the expansion of Nkx2.2 expression. Asterisk in (F) indicates the position of prethalamus. (C)–(F) are stained with DAPI.

(G–M) Chimeras immunoreacted for Gsx2 and Islet1 containing either (G and H) a high or (I–M) a low proportion of mutant cells. Arrows point to the same cell in (I) and (M).

Scale bars, 400 μm (A), 200 μm (C–F), and 100 μm (H, I, L, and M). See also Figure S1.

size and patterning (Grindley et al., 1997; Pratt et al., 2000, 2002; Warren and Price, 1997).

In the past, it has been considered that Pax6 functions downstream of Shh, which represses Pax6 (Ericson et al., 1997; Macdonald et al., 1995; Robertshaw et al., 2013), but it has also been reported that loss of Pax6 increases the size of the Shh-producing ZLI (Grindley et al., 1997; Pratt et al., 2000; Chatterjee et al., 2014), suggesting that Pax6 might somehow regulate *Shh*. We examined the influence of Pax6 on diencephalic patterning and identified an important cell-autonomous action of Pax6 on the expression of *Shh*. Our findings indicate a crucial role for mutual repression between Pax6 and Shh in diencephalic cell specification.

RESULTS

In normal E12.5 mice, Pax6 expression is highest in the progenitor and postmitotic layers of the prethalamus, absent along the thalamic/prethalamic border, and distributed in a gradient through the progenitor layer of the thalamus (lowest near to the ZLI) (Figure 1A). We examined the consequences of Pax6 absence for patterning in each of these regions (Figure 1B).

Pax6 Is Required Cell Autonomously for Normal Prethalamic Identity

A marker of prethalamic progenitors, Gsx2, was undetectable in *Pax6*$^{-/-}$ diencephalon (Figures 1C and 1D), and numbers of Islet1+ cells were greatly reduced in prethalamic postmitotic cells (asterisk in Figure 1D). The absence of Gsx2-expressing lineages was shown using a cre recombinase transgene controlled by the Gsx2 promoter (Kessaris et al., 2006) with a floxed-stop-GFP reporter (Miyoshi et al., 2010). In controls, most prethalamic cells expressed GFP (Figure 1E), consistent with their descent from Gsx2+ prethalamic progenitors, but no GFP+ cells were detected in an equivalent region of *Pax6*$^{-/-}$ mutants (asterisk in Figure 1F).

To test whether Pax6 is required cell autonomously for expression of Gsx2 by prethalamic cells, we generated *Pax6*$^{-/-}$ ↔ *Pax6*$^{+/+}$ chimeras. The contributions of *Pax6*$^{-/-}$ cells to each chimera varied (nine chimeras were analyzed), allowing us to analyze situations in which mutant cells were surrounded by much larger numbers of wild-type cells and those where the opposite was the case. In all, *Pax6*$^{-/-}$ cells contributed to the prethalamus.

In chimeras with a high contribution of mutant cells, none of these cells expressed Gsx2, whereas even small clusters of wild-type prethalamic progenitors embedded among them retained Gsx2 expression (Figure 1H). Similarly, in chimeras with a low contribution of mutant cells, all *Pax6*$^{-/-}$ progenitors were Gsx2−, even those in very small isolated groups (Figures 1I–1M), whereas all wild-type progenitors, even individually isolated ones, were Gsx2+ (Figures 1L and 1M). In low-contribution chimeras, Islet1 was expressed by most *Pax6*$^{-/-}$ cells (as it was by most wild-type cells) exiting the progenitor layer (Figure 1M), but in high-contribution chimeras, it was expressed by a smaller proportion (about 50%) of differentiating cells (Figure 1G).

These results indicate that cells in the prethalamus have an absolute cell-autonomous requirement for Pax6 in order to express Gsx2. Pax6 is not required for prethalamic Islet1 expression, although the observation that proportions of Islet1+ cells are reduced when large proportions of prethalamic cells are *Pax6*$^{-/-}$ suggests a non-cell-autonomous effect of extensive Pax6 loss on prethalamic Islet1 expression.

Loss of Pax6 Causes Expansion of Domains around the Prethalamic/Thalamic Border

In normal diencephalic development, Nkx2.2 expression marks a thin strip of cells around the prethalamic/thalamic border, including progenitors around the ZLI that coexpress Olig3 (Figure 2A) and postmitotic cells extending through the neuroepithelial wall to the developing vLG (Figures 1E and 2A; Kitamura et al., 1997; Scholpp and Lumsden, 2010; Vue et al., 2007). In *Pax6*$^{-/-}$ diencephalon, this domain was greatly expanded (double arrow in Figure 1F; Figure 2B); it still reached a collection of superficially located Nkx2.2+ cells in the same relative position as the vLG of normal embryos (arrowheads in Figure 2B). The domains of *Lhx1* and *Lhx5* expression in postmitotic cells around the prethalamic/thalamic border were also greatly enlarged in *Pax6*$^{-/-}$ embryos (Figures 2C–2F, S1A, and S1B).

We tested whether the mechanism of expansion of these domains of expression involved incorrect cellular specification, causing an abnormally broad swathe of cells, many of which would normally have adopted distinct thalamic or prethalamic identities, to take on the identities of cells normally located very close to the prethalamic/thalamic border. Ngn2+ lineage cells, which populate the thalamus of wild-type and *Pax6*$^{-/-}$ embryos (Figures 2I and 2J), were labeled using a transgene expressing a tamoxifen-inducible cre recombinase, creER, under the control of the *Ngn2* promoter (Zirlinger et al., 2002) and a floxed-stop-GFP reporter allele (Miyoshi et al., 2010). Pregnant females received tamoxifen at E10.5 so as to induce reporter activation by E12.5 (Kessaris et al., 2006), and embryos were collected at E14.5. In E14.5 controls, GFP+ cells were present throughout the body of the thalamus, and their axons could be seen exiting through the prethalamus; Ngn2 lineage cells close to the thalamic/prethalamic border did not express Lhx1/Lhx5 (Figures 2I and 2K). In E14.5 *Pax6*$^{-/-}$ embryos, about 75% of the GFP+ cells located in the rostral part of the thalamus were double labeled for Lhx1/Lhx5 (Figures 2J and 2L; cells were counted in three sections from each of three embryos), providing evidence for the misspecification of many postmitotic cells in this region.

Examination of the thalamus in *Pax6*$^{-/-}$ embryos showed an overall reduction in its size (as marked by Sox2, *Gbx2*, and *Ngn2* expression: Figures 1E, 1F, 2C, 2D, and S1C–S1F) but an expansion of the part of its progenitor domain closest to the ZLI at E12.3–E13.5 (Figures 2E–2H, 2M, 2N, S1G, S1H, and S2). This region, known as pTh-R (Inamura et al., 2011; Suzuki-Hirano et al., 2011; Vue et al., 2007; Jeong et al., 2011), expresses *Ascl1*, *Gsx1*, and *Nkx2.2* but only low levels of *Ngn2*, and its expansion in *Pax6*$^{-/-}$ embryos coincides with a reduction in the size of the pTh-C, the caudal region of thalamic progenitors, which expresses *Ngn2*.

Previous studies showed that pTh-R contributes GABAergic neurons (Vue et al., 2007). Our analysis of postmitotic GABAergic neurons (*VGAT* and *Gad67*) and glutamatergic neurons (*mGluR1*) confirmed shrinkage of the glutamatergic population in caudal thalamus and expansion of the GABAergic population in rostral thalamus (Figures S3A–S3I). Expression of Six3 in a small group of very rostral postmitotic thalamic cells was also expanded in *Pax6*$^{-/-}$ mutants (Figures S3J–S3L, arrows). These findings indicate that the absence of Pax6 results in expansion of both pTh-R and the GABAergic population of cells that it generates at the expense of the glutamatergic pTh-C-derived population.

Mis-Patterning of Pax6$^{-/-}$ Cells in Rostral Thalamus Is Conditional

The fact that Pax6 is expressed more strongly in pTh-C than pTh-R progenitors and that rostral territory expands if Pax6 is lost suggests that Pax6 in pTh-C normally suppresses the molecular phenotype associated with the rostral thalamus. To begin addressing how Pax6 suppresses the rostral thalamic phenotype, we tested whether its requirement is cell autonomous by examining the expression of rostral thalamic markers in *Pax6*$^{-/-}$ ↔ *Pax6*$^{+/+}$ chimeras.

Figure 3 shows examples of chimeras containing high or low proportions of *Pax6*$^{-/-}$ (GFP+) cells. Regardless of the balance of wild-type and mutant cells, the boundary region between

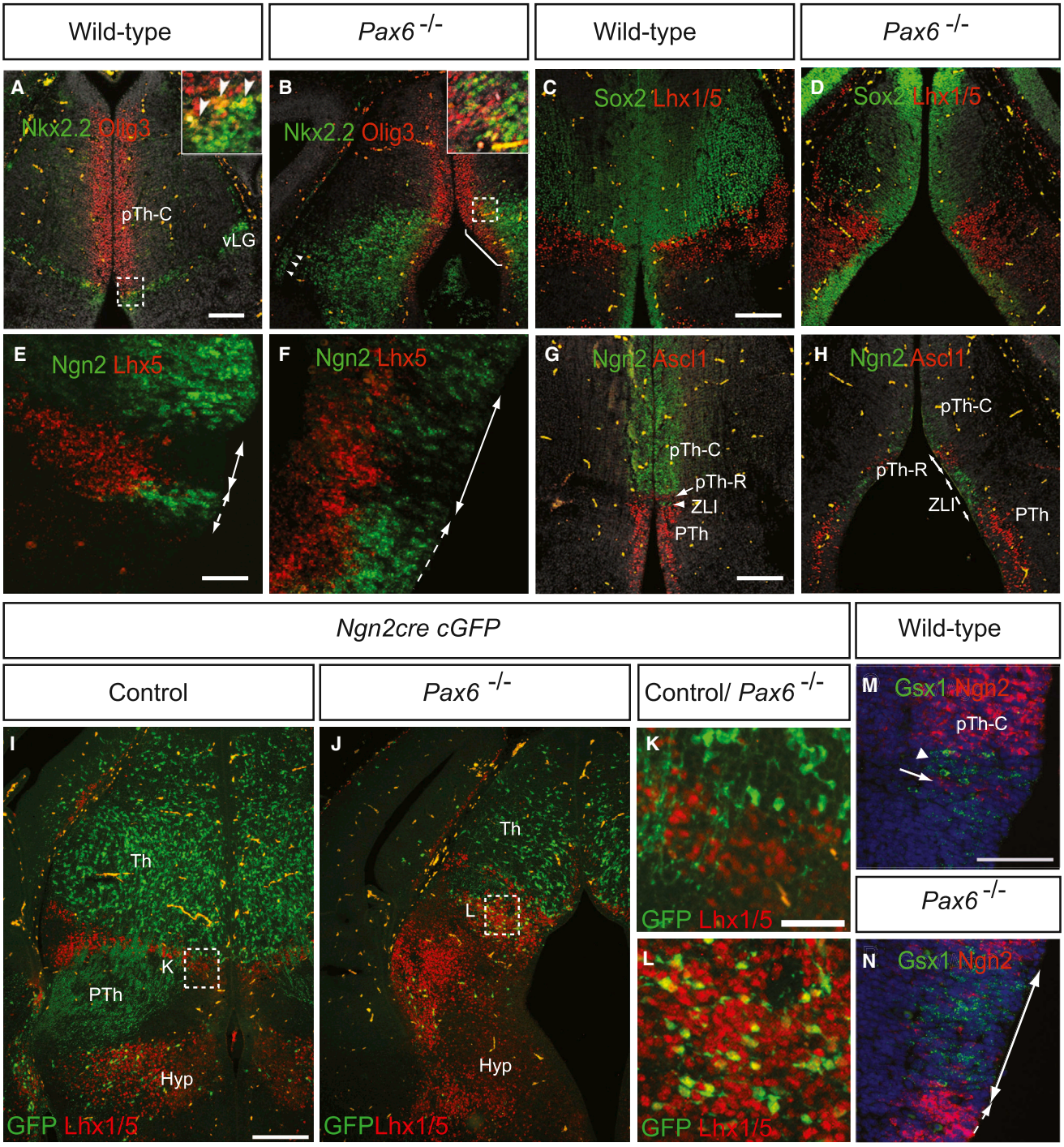

Figure 2. Expansion of Domains Close to the Thalamic/Prethalamic Border due to Cellular Misspecification

(A–H) Immunohistochemistry at E13.5. Insets in (A) and (B) show higher-magnification views of boxed areas. Arrowheads in (A) point to examples of double-labeled cells. Bracket in (B) indicates position of expanded thalamic/prethalamic border region. Arrowheads in (B) point to the equivalent of vLG. Broken double arrows point to the position of ZLI. Solid double arrows point to the position of pTh-R in (E), (F), and (H).

(I–L) Immunohistochemistry at E14.5 for Lhx1/Lhx5 and GFP expression (induced in *Ngn2cre*^{ER} embryos by tamoxifen at E10.5). Hyp, hypothalamus. (K) and (L) are enlargements of the boxed areas in (I) and (J).

(M and N) *Gsx1* expressed in pTh-R (arrowhead/solid double arrow) and *Ngn2* in the ZLI (arrow/broken arrow) at E12.5.

Scale bars, 100 μm (A–D, G, and H), 50 μm (E, F, K, and L), 200 μm (I and J), and 75 μm (M and N). See also Figure S2.

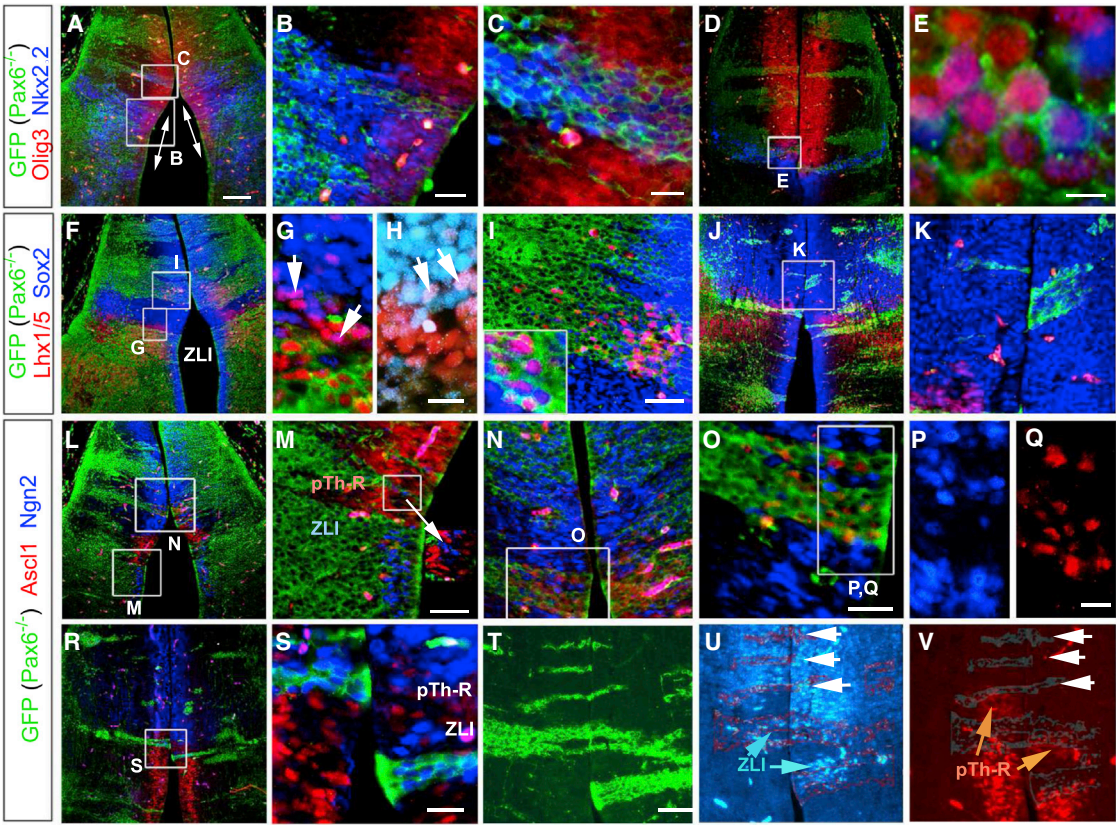

Figure 3. Mis-Patterning of *Pax6*$^{-/-}$ Cells in Chimeras Depends on Their Number and Location

Sections are from E13.5 chimeras comprising *Pax6*$^{-/-}$ cells (GFP+) mixed with *Pax6*$^{+/+}$ cells (except H).

(A–C, F–I, and L–Q) Chimeras with high contributions of mutant cells. (H) A nonchimeric wild-type section is shown. Arrows in (G) and (H) point to double-labeled cells. Inset in (I) shows *Pax6*$^{-/-}$ thalamic cells labeled with Lhx1/Lhx5 and Sox2. Inset in (M) shows that, close to the ZLI, *Pax6*$^{-/-}$ cells express Ngn2, and abnormally large numbers of wild-type cells express Ascl1.

(D, E, J, K, and R–V) Chimeras with low contributions of mutant cells. Boxed areas are shown in higher-magnification panels marked beside each. Double-headed arrows in (A) point to the extent of Olig3 and Nkx2.2 coexpression corresponding to expanded ZLI and pTh-R of *Pax6*$^{-/-}$ mutants. The pattern of *Pax6*$^{-/-}$ cells in (T) is indicated lightly on (U) and (V). Those in the thalamus (arrows) are Ngn2+ Ascl1−, as are their wild-type neighbors.

Scale bars, 150 μm (A, D, F, J, L, and R), 50 μm (B, I, K, M, N, and T–V), 25 μm (C, G, H, P, Q, and S), 10 μm (E), and 40 μm (O). See also Figure S4.

the prethalamus and thalamus was always identifiable. Its progenitor layer contained cells that were both Olig3+ and Nkx2.2+ (Figures 3A, 3B, 3D, and 3E), and the overlying mantle zone contained Nkx2.2+ cells (Figures 3A and 3D) and Lhx1/Lhx5+ cells (Figure 3F), whose expression overlapped slightly with that of thalamic Sox2 expression as occurs in wild-type embryos (Figures 3G and 3H). Both wild-type and *Pax6*$^{-/-}$ cells contributed to this boundary region, which was broader in those chimeras that contained a high proportion of mutant cells (marked by double-headed arrows in Figure 3A).

Nkx2.2, Lhx1/Lhx5, and Ascl1 are not normally expressed through the body of the thalamus, but they were expressed by some thalamic *Pax6*$^{-/-}$ cells in chimeras. Examples are shown in Figures 3A, 3C, 3F, 3I, 3L, and 3N–3Q. Interestingly, the mutant thalamic cells that showed abnormal expression of Nkx2.2, Lhx1/Lhx5, and Ascl1, which their surrounding wild-type neighbors did not, were all located relatively close to the thalamic/prethalamic border (within about 100–200 μm) in clusters of 100–200 cells or more (Figures 3A, 3C, 3F, 3I, 3L, and 3N–3Q). Even large clusters of *Pax6*$^{-/-}$ cells more distant from the border expressed the same markers as their wild-type neighbors (Figures 3A, 3F, 3I, 3L, and 3N). Smaller clusters of *Pax6*$^{-/-}$ cells always showed the same expression as their wild-type neighbors (Figures 3D, 3J, 3K, and 3R–3V). These findings indicate that absence of Pax6 does not cause a straightforward cell-autonomous upregulation of the rostral thalamic phenotype (Nkx2.2+, Lhx1/Lhx5+, and Ascl1+). Although mutant cells do upregulate rostral thalamic markers in some circumstances, they need to be in a critical mass relatively close to the thalamic/prethalamic border.

Another revealing result was that in chimeras containing a high contribution of mutant cells, we observed expanded Ascl1 domains immediately caudal to the expanded *Pax6*$^{-/-}$ ZLI (i.e., corresponding to expanded pTh-R) that comprised wild-type cells, providing clear evidence for a non-cell-autonomous upregulation of Ascl1 and loss of Ngn2 around the expanded mutant ZLI (Figures 3L and 3M). In summary, our findings strongly suggest that a major underlying cause of abnormal thalamic

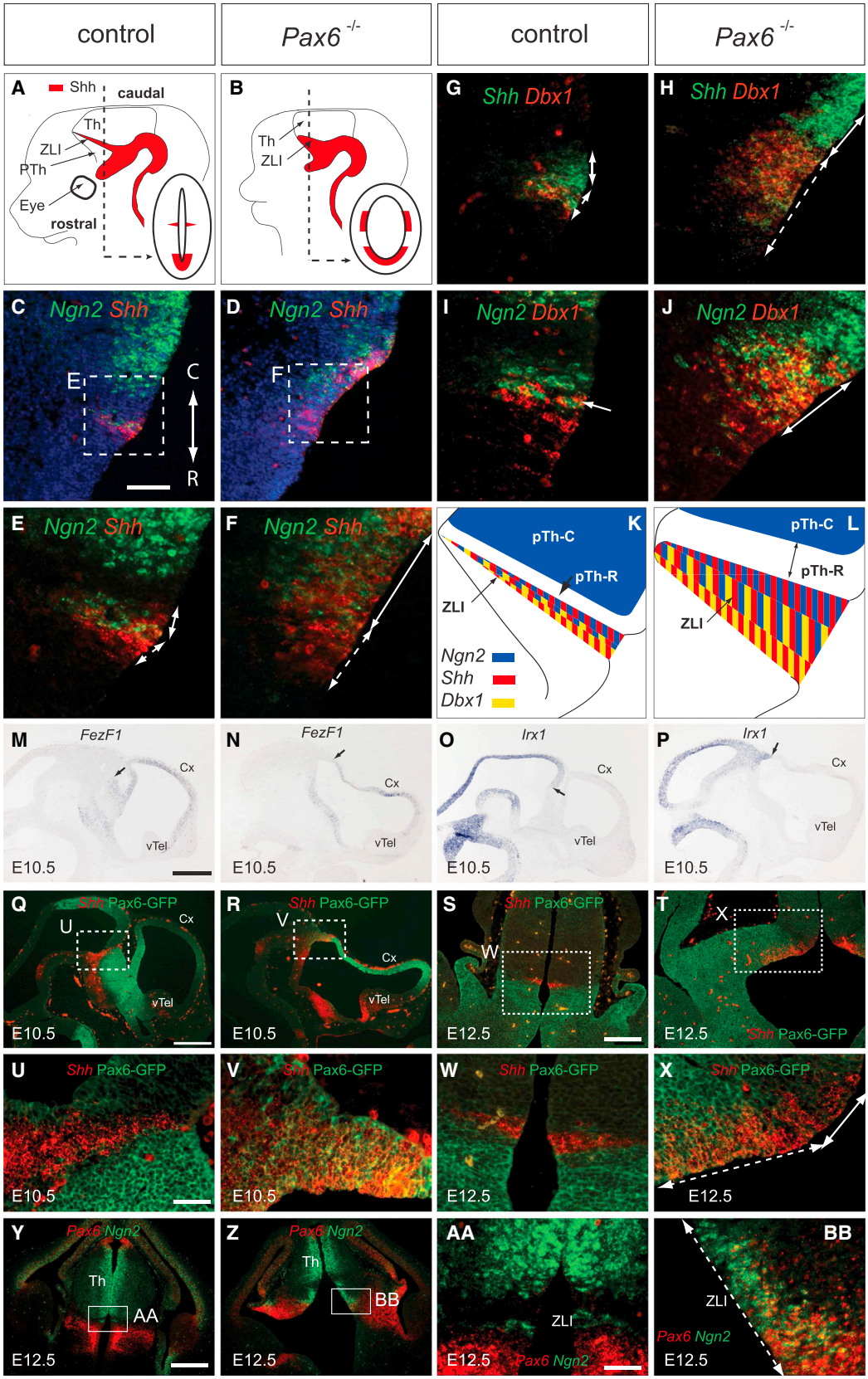

(legend on next page)

patterning in the absence of Pax6 is a position-dependent defect of local intercellular signaling. This contrasts with the absolute cell-autonomous requirement for Pax6 for Gsx2 expression in prethalamus described above.

Expansion of the ZLI and Its Subdivisions in Pax6$^{-/-}$ Mutants

Position-dependent defects of signaling among cells around the thalamic/prethalamic border might be caused by defects of the ZLI. We compared the expression of markers of the ZLI in control and *Pax6*$^{-/-}$ embryos using in situ hybridization and immunofluorescence at E12.5–E13.5. The wild-type E12.5 ZLI is a thin *Shh*-expressing wedge-shaped structure in the alar plate (Figure 4A). Close to its tip, it appears as a single line of cells expressing both *Shh* and *Ngn2* (Vue et al., 2007). We found, however, that as it widens toward its base (e.g., at the level of the broken line in Figure 4A), only its caudal part expresses both *Ngn2* and *Shh* (Figure 4C; solid double-headed arrow in Figure 4E). Its rostral part expresses *Dbx1* (broken double-headed arrow in Figure 4G), and a central domain is both *Dbx1*+ and *Ngn2*+ (arrow in Figure 4I; summarized in Figure 4K).

In E12.5 *Pax6*$^{-/-}$ mutants, there was a large rostrocaudal expansion of *Shh* expression in the alar plate in a location equivalent to that of the ZLI (Figures 4B, 4D, 4F, 4H, 4J, and 4L). This was divisible into an enlarged caudal domain expressing both *Shh* and *Ngn2* (solid double-headed arrow in Figure 4F) and an enlarged rostral domain expressing both *Shh* and *Dbx1* (broken double-headed arrow in Figure 4H) with an enlarged central domain expressing *Dbx1* and *Ngn2*+ (double-headed arrow in Figure 4J). These results indicate that, in the absence of Pax6, the ZLI and its subdomains, identified by expression/coexpression of *Shh*, *Ngn2*, and *Dbx1*, are enlarged, as summarized in Figures 4K and 4L. The *Pitx2*-expressing mantle zone immediately superficial to the ZLI is also expanded in *Pax6*$^{-/-}$ mutants (Figures S3M–S3O).

Expansion of the ZLI Is Caused by Misspecification of Cells around the Thalamic/Prethalamic Boundary

We then tested whether the expansion of the ZLI in *Pax6*$^{-/-}$ mutants results from the misspecification of cells flanking the normal position of the ZLI (e.g., rather than an overproliferation of correctly specified ZLI progenitors). The normal ZLI develops at about E9.5–E10.5 in the mouse at the interface between a rostral diencephalic *FezF1*+ domain (Figure 4M) and a caudal diencephalic *Irx1*+ domain (Figure 4O) (Hirata et al., 2006). It comprises *Shh*+ cells sandwiched between *Pax6*+ domains rostral and caudal to it (Figures 4Q and 4U). We tested whether expansion of the ZLI in *Pax6*$^{-/-}$ embryos involves the erroneous activation of *Shh* by flanking cells expressing the *Pax6* gene. We used two approaches to identify the *Pax6*+ cells in *Pax6*$^{-/-}$ mutants. In the first, they were labeled by GFP produced from a Pax6-yeast artificial chromosome-reporter transgene that expresses GFP in *Pax6*-expressing cells regardless of whether they are *Pax6*$^{-/-}$ or not (*Pax6*-GFP; Tyas et al., 2006). In the second, we identified *Pax6*+ cells by in situ hybridization.

In E10.5 *Pax6*$^{-/-}$ embryos, the boundary between *FezF1* and *Irx1* expression was as clear as in controls (arrows in Figures 4M–4P), indicating that Pax6 is not required for this early patterning and allowing us to identify the position of ZLI formation. We examined expression of *Shh* and *Pax6*-GFP at this position in E10.5 *Pax6*$^{-/-}$ embryos. In complete contrast to controls (Figures 4Q and 4U), we observed a relatively large block of tissue whose cells coexpressed high levels of *Pax6*-GFP and *Shh* (Figures 4R and 4V). This tissue was largely caudal to the position marked for ZLI development by the interface of *FezF1*+ and *Irx1*+ territories (compare Figures 4N and 4P with Figures 4R and 4V).

Normally, the difference in *Pax6* expression between prethalamus (high) and thalamus (low) becomes greater by E12.5, as shown by expression of *Pax6*-GFP in Figures 4S and 4W. As at E10.5, in E12.5 *Pax6*$^{-/-}$ embryos (Figures 4T and 4X), the caudal part of the abnormally broad *Shh*+ domain extended abnormally far into the low *Pax6*-GFP-expressing thalamic progenitor layer (double-headed arrow in Figure 4X). The rostral part of the abnormally broad *Shh*+ domain overlapped the region of high *Pax6*-GFP prethalamic expression (broken double-headed arrow in Figure 4X), with cells in this region being double positive for *Shh* and *Pax6*-GFP expression. At E12.5, we also observed abnormal coexpression of *Pax6* and *Ngn2* mRNAs in this rostrally extended part of the expanded *Pax6*$^{-/-}$ ZLI (Figures 4Y–4BB). Whereas *Ngn2* and *Pax6* expression is normally complementary at E12.5 (with Ngn2 in the ZLI and high Pax6 rostral to it; Figures 4Y and 4AA), in *Pax6*$^{-/-}$ embryos, many *Ngn2*+ cells in the expanded ZLI coexpress high levels of *Pax6* (Figures 4Z and 4BB). These findings indicate that *Pax6*$^{-/-}$ progenitor cells rostral and caudal to the position of normal ZLI formation are misspecified.

Misregulation of Shh Expression by Cells around the ZLI Is Cell Autonomous

The failure of cells around the thalamic/prethalamic border to repress *Shh* expression in *Pax6*$^{-/-}$ embryos might provide an explanation for aspects of the mis-patterning of this region in terms of its abnormal marker-gene expression in *Pax6*$^{-/-}$

Figure 4. ZLI Expansion and Misspecification of Surrounding Cells in *Pax6*$^{-/-}$ Embryos

(A and B) Expression of Shh in parasagittal and coronal planes at E12.5. Broken lines indicate planes of coronal sections.

(C–J) Double in situ hybridizations on coronal sections at E12.5. (C–F) *Shh* and *Ngn2* overlap in caudal (C) ZLI (solid double arrows in E and F), and not rostral (R) ZLI (broken double arrows in E and F). (G and H) *Shh* and *Dbx1* overlap in rostral ZLI (broken double arrows), and not caudal ZLI (solid double arrows). (I and J) *Ngn2* and *Dbx1* overlap only in central ZLI (arrow/double arrow).

(K and L) Summary diagrams.

Scale bars, 100 μm (C–J). See also Figure S3.

(M–P) Expression of *FezF1* and *Irx1* in sagittal sections. Arrows point to the position of ZLI formation (note the ventricular expansion in mutants).

(Q–X) Expression of *Shh* and a Pax6-GFP reporter. *Shh* and *Pax6* overlap rostral and caudal to the position of the ZLI in mutants (broken and solid double arrows in X).

(Y–BB) Expression of *Pax6* and *Ngn2*. Coexpression in mutants is shown by broken double arrow in (BB).

Cx, cortex; Th, thalamus; vTel, ventral telencephalon. Scale bars, 200 μm (M–R, Y, and Z), 150 μm (S and T), and 50 μm (U–X, AA, and BB). See also Figure S7.

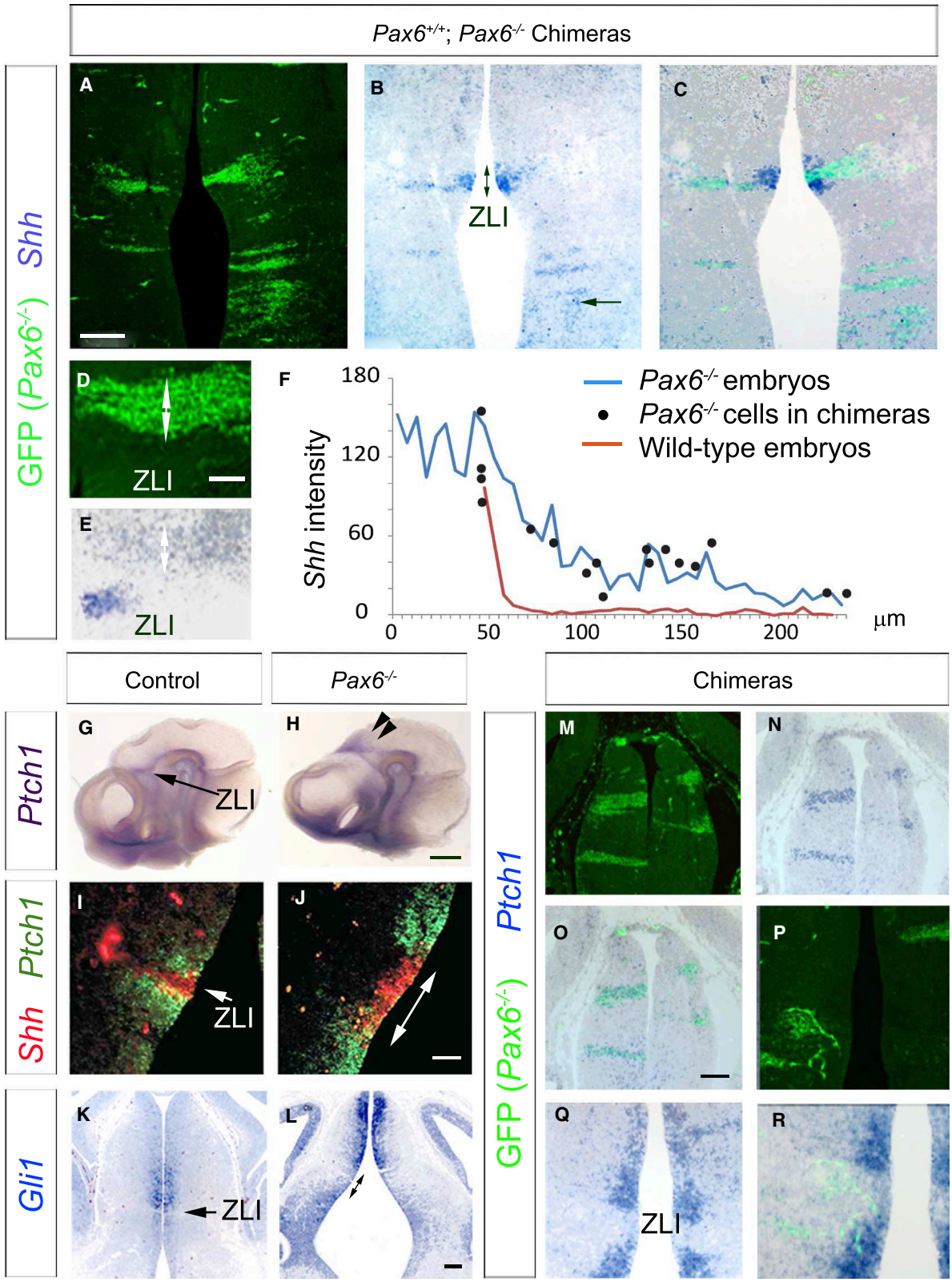

Figure 5. Cell-Autonomous Upregulation of *Shh* in the *Pax6*$^{-/-}$ Diencephalon

(A–E) E13.5 chimeras. *Pax6*$^{-/-}$ cells are GFP+. *Shh* mRNA expression is shown by in situ hybridization. Arrow in (B) and double-headed arrow in (D) and (E) point to clusters of mutant cells expressing *Shh*. (C) is (A) and (B) combined.

(legend continued on next page)

embryos and chimeras. To test this, we first examined chimeras to discover whether the abnormal upregulation of *Shh* in *Pax6*$^{-/-}$ cells around the thalamic/prethalamic border is cell autonomous. We focused on chimeric embryos in which small minorities of *Pax6*$^{-/-}$ cells were surrounded by vast majorities of wild-type cells, in which influences from outside *Pax6*$^{-/-}$ cell groups should be relatively normal.

In chimeras, small clusters of *Pax6*$^{-/-}$ (GFP+) cells throughout the diencephalon all expressed *Shh* regardless of their size and whether they were in the ZLI, thalamus, or prethalamus (Figures 5A–5E). There was systematic variation in their levels of *Shh*. Cells embedded in the ZLI expressed *Shh* at levels that were indistinguishable from those of their *Shh*-expressing wild-type neighbors (Figures 5A–5C). Outside the ZLI, *Pax6*$^{-/-}$ cells achieved levels of *Shh* expression that, although raised above those of their wild-type neighbors, were lower than those of cells in the ZLI (e.g., horizontal arrow in Figure 5B, and double-headed arrows in Figures 5D and 5E). We measured the relative intensities of *Shh* labeling across the diencephalon of wild-type and *Pax6*$^{-/-}$ embryos and in the clusters of *Pax6*$^{-/-}$ cells in chimeras. The relationship between intensity and distance from the ZLI was very similar in *Pax6*$^{-/-}$ mutants and in *Pax6*$^{-/-}$ cells in chimeras (Figure 5F).

In control chimeras comprising a mixture of *Pax6*$^{+/+}$ and *Pax6*$^{+/+}$ GFP-expressing cells, the GFP+ cells were not clustered but were scattered throughout the diencephalon, the in situ hybridization staining for *Shh* appeared normal, and there was no evidence that levels of *Shh* depended on whether cells were GFP+ or not (Figures S4A–S4C).

These findings indicate that *Pax6*$^{-/-}$ diencephalic cells activate *Shh* cell autonomously because activation occurred even when mutant cells were embedded in an environment comprising a large majority of wild-type cells. Moreover, the results suggest that the mechanism that sets the level of activation with reference to distance from the ZLI in the absence of Pax6 acts cell autonomously because the relationship between the locations of the *Pax6*$^{-/-}$ patches and their levels of *Shh* expression reflected the relationship in *Pax6*$^{-/-}$ embryos. These results have the potential to explain the observed mis-patterning of those *Pax6*$^{-/-}$ cells close to the thalamic/prethalamic border in *Pax6*$^{-/-}$ mutants and chimeras. They might also explain the expanded Ascl1 domain affecting wild-type cells close to the border (Figures 3L and 3M) and the lack of repatterning among wild-type cells further from the border. We do not exclude the possibility that factors other than levels of *Shh* expression might also be important in region-specific repatterning.

Ptch1 Is Activated in Pax6$^{-/-}$ Diencephalic Cells except Those within the ZLI

Previous studies have shown that expression of *Ptch1* and *Gli1* can be upregulated by Shh signaling and is normally high in cells adjacent to the ZLI (Figures 5G, 5I, and 5K; Bai et al., 2002, 2004; Gajović et al., 1997; Goodrich et al., 1996; Kiecker and Lumsden, 2004; Lee et al., 1997; Marigo and Tabin, 1996; Wijgerde et al., 2002; Vue et al., 2009). We tested the prediction that if the abnormal *Shh* expression of *Pax6*$^{-/-}$ cells has functional consequences for those cells, then they should upregulate *Ptch1* and *Gli1*. In situ hybridizations on E10.5 *Pax6*$^{-/-}$ whole mounts showed that staining for *Ptch1* spread more broadly than normal through surrounding diencephalic tissue (arrowheads in Figures 5G and 5H). Coronal sections of E12.5–E13.5 *Pax6*$^{-/-}$ embryos showed expansion of the *Ptch1*+ areas and abnormally strong *Gli1* expression in the thalamus and prethalamus (Figures 5I–5L). We then examined the expression of *Ptch1* in *Pax6*$^{+/+}$ ↔ *Pax6*$^{-/-}$ chimeras. Outside the ZLI, clusters of *Pax6*$^{-/-}$ (GFP+) cells were *Ptch1*+ (Figures 5M–5O), indicating a response to the Shh that they produce. Wild-type cells surrounding the ZLI were *Ptch1*+, as in normal embryos (Figures 5Q and 5R).

Interestingly, *Ptch1* and *Gli1* are normally downregulated within areas of high *Shh* expression in the ZLI and basal plate (Figures 5G, 5I, and 5K; Marigo and Tabin, 1996). *Ptch1* and *Gli1* are also downregulated in the expanded ZLI of *Pax6*$^{-/-}$ embryos (Figures 5J and 5L) and by *Pax6*$^{-/-}$ cells embedded in the ZLI in chimeras (Figures 5P–5R). To test whether this might also be caused by exposure to high levels of Shh, we administered vismodegib (GDC-0449), a selective inhibitor of the Shh receptor Smo (expressed throughout control and *Pax6*$^{-/-}$ diencephalon; Figures S5A and S5B), to *Pax6*$^{-/-}$ embryos. This treatment caused a dose-dependent overall reduction of the area of *Ptch1* expression but an upregulation of *Ptch1* at the expanded Shh+ *Pax6*$^{-/-}$ ZLI (Figures S5C–S5F), in agreement with the hypothesis above.

In the forebrain, Pax6 is also strongly expressed in the cerebral cortex, and a previous microarray-based analysis found small but significant upregulation of both *Shh* and *Ptch1* in cortical cells from *Pax6*$^{-/-}$ embryos (*Shh*: +1.38-fold, p = 0.038; *Ptch1*: +1.36-fold, p = 0.043; Mi et al., 2013). In situ hybridization on *Pax6*$^{-/-}$ embryos did not show obvious upregulation of *Shh* or *Ptch1* (Figures S4D–S4G), but in chimeras, where mutant and wild-type cells are together in the same sections, we did detect slightly stronger staining for *Shh* and *Ptch1* in *Pax6*$^{-/-}$ cells (Figures S4H–S4K). These findings indicate that Pax6 also has a cell-autonomous repressive effect on *Shh* in cortex, although its magnitude appears less than in diencephalon.

Pax6 Regulates Diencephalic Patterning by Controlling Shh Signaling

We then tested whether abnormalities of diencephalic patterning in *Pax6*$^{-/-}$ embryos result from abnormally high Shh signaling around the ZLI, by administering vismodegib (GDC-0449) to inhibit Shh signaling in *Pax6*$^{-/-}$ embryos. We examined the

(F) Intensity of Shh staining above background (measured in ImageJ) with distance from the center of the ZLI. Because the ZLI of *Pax6*$^{-/-}$ embryos is expanded, data from groups of *Pax6*$^{-/-}$ cells in chimeras and from wild-types are offset by ~50 μm to allow comparisons of relationships in surrounding tissue (n = 3 embryos of each type; data from nonchimeric embryos are averages).
(G and H) *Ptch1* in situ hybridization at E10.5. Arrowheads point to an expanded mutant domain.
(I–L) Sections at E12.5 (I and J) and E13.5 (K and L). Double-headed arrows point to mutant ZLI.
(M–R) E13.5 chimeras. (O) is (M) and (N) combined. (R) is (P) and (Q) combined.
Scale bars, 100 μm (A–C and K–R), 50 μm (D, E, I, and J), and 500 μm (G and H). See also Figure S5.

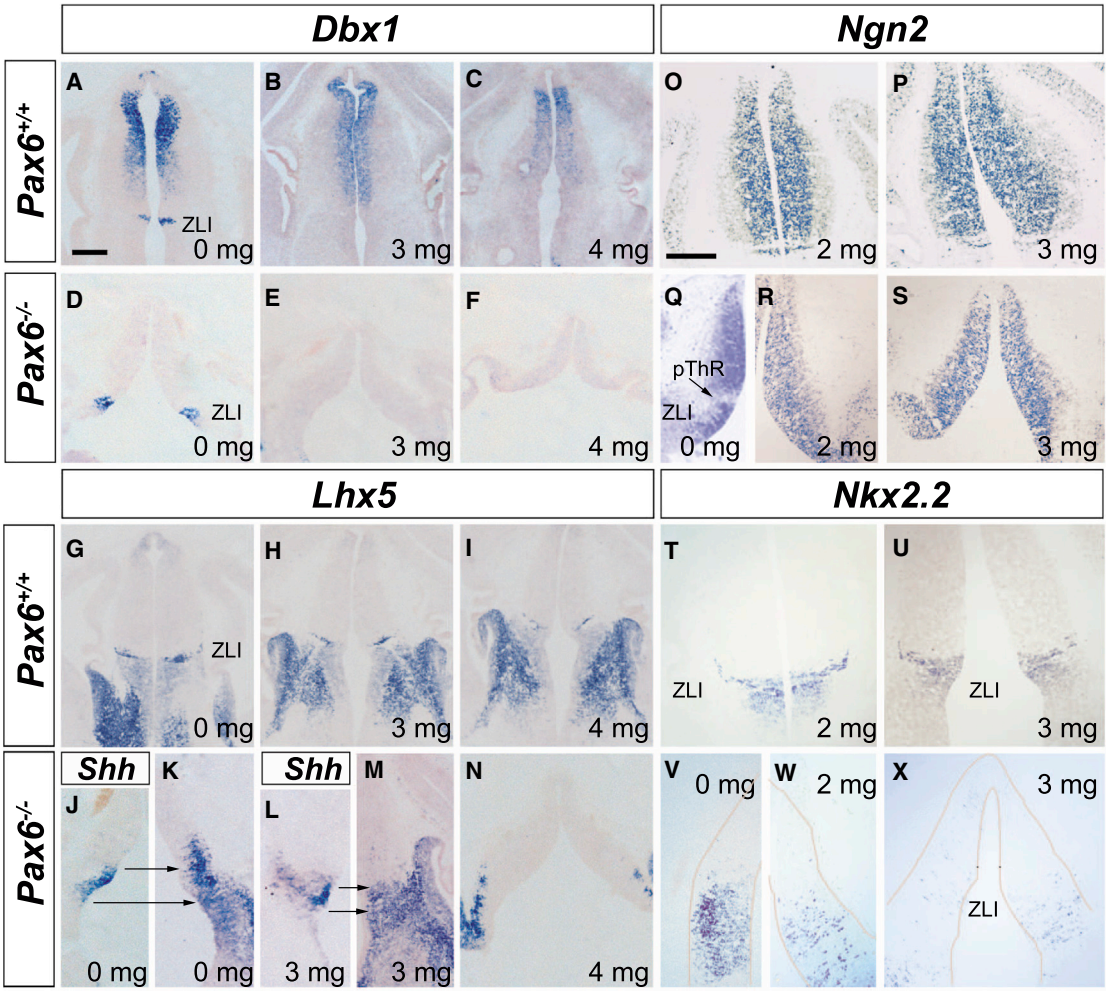

Figure 6. Shh Blockade Affects *Pax6*$^{-/-}$ Diencephalic Patterning

(A–X) Expression of *Dbx1* (A–F), *Lhx5* (G–N), *Ngn2* (O–S), and *Nkx2.2* (T–X) mRNAs in wild-type and *Pax6*$^{-/-}$ E12.5 embryos treated with vismodegib (doses on each panel).

(J–M) The position of expanded mutant ZLI is indicated by analysis of *Shh* expression in adjacent sections (arrows). Shh expression is not altered by vismodegib; Ptch1 expression is (Figure S5).

Scale bars, 250 μm (A–N) and 200 μm (O–X). See also Figure S6.

effects of Shh blockade on markers whose expression is altered at or around the ZLI and the thalamic/prethalamic border in *Pax6*$^{-/-}$ mutants (*Dbx1*, *Ngn2*, *Lhx5*, *Nkx2.2*, and *Ascl1*).

In wild-types, *Dbx1* is expressed in the ZLI and in a gradient through the thalamus (Figures 4G, 4I, 4K, and 6A), whereas in *Pax6*$^{-/-}$ mutants, its expression is expanded at the ZLI and greatly reduced in the thalamus (Figures 4H, 4J, 4L, and 6D). Its expression at the ZLI was abolished by administration of vismodegib, both in wild-types and *Pax6*$^{-/-}$ embryos (Figures 6B, 6C, 6E, and 6F), indicating that its expression/expanded expression in this region is dependent on Shh.

In wild-types, the intensity of staining for *Lhx5* expression around the thalamic/prethalamic border declined with increasing doses of vismodegib, but otherwise, the pattern of expression appeared unaffected (Figures 6G–6I). In *Pax6*$^{-/-}$ mutants, the expanded domain of intense *Lhx5* expression around the thalamic/prethalamic border (whose position was recognized by Shh expression in adjacent sections) was reduced by increasing doses of vismodegib (Figures 6J–6N), indicating the importance of Shh signaling for this aspect of the mutant phenotype.

The pattern of *Ngn2* expression in wild-types appeared unaffected by treatment with vismodegib, showing high expression in the thalamus and ZLI with reduced expression in pTh-R (Figures 6O and 6P). In *Pax6*$^{-/-}$ mutants, however, the region of low *Ngn2* expression at the pTh-R was no longer visible after vismodegib treatment (Figures 6Q–6S). Ascl1 has a complementary expression pattern to that of *Ngn2*: wild-types show high expression in pTh-R and prethalamus and low expression in the ZLI and thalamus (Figures 2G and S6A), whereas *Pax6*$^{-/-}$ mutants show expanded expression at the pTh-R (Figures 2H and S6B). Vismodegib had no obvious effect on the Ascl1

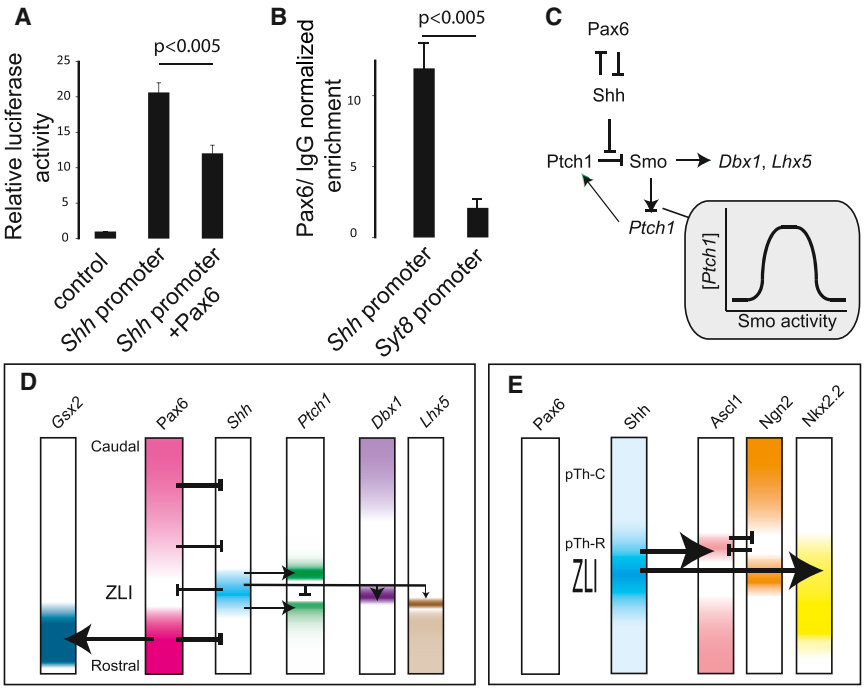

Figure 7. Effects of Pax6 on *Shh* and Diencephalic Patterning

(A) Results of luciferase assays (firefly relative to Renilla luciferase activity). Activity of the *Shh* promoter is repressed by Pax6 (n = 5 independent assays; Student's t test).

(B) The results of quantitative ChIP to test for enrichment of *Shh* or *Syt8* (Pax6 nonbound control) promoter fragments. Mean ± SEM is shown (n = 3) of fold enrichments with Pax6 antibody relative to IgG control (Student's t test).

(C and D) A model to explain our data. Pax6 represses *Shh* in the diencephalon and is repressed by Shh at the ZLI. Shh derepresses Smo (Taipale et al., 2002), thereby activating *Dbx1* and *Lhx5* and having a biphasic effect on *Ptch1* expression. Pax6 cell autonomously activates *Gsx2* in prethalamus.

(E) When Pax6 is absent, *Shh* expression is upregulated, thereby increasing Nkx2.2 expression, increasing Ascl1 expression in pTH-R, and causing a complementary decrease of Ngn2 in this region.

expression pattern in wild-types (Figure S6C) but caused a marked loss of expression at the pTh-R of *Pax6*$^{-/-}$ mutants (Figure S6D), reducing both the area containing Ascl1+ cells and their density (from 20.5 ± 1.9 SEM, n = 3, to 9.78 ± 1.8, n = 3, cells per 0.005 mm^2; $p < 0.05$, Student's t test). Vismodegib had little effect on *Nkx2.2* expression in wild-types (Figures 6T, 6U, and 2A), but it reduced substantially the expanded *Nkx2.2* expression around the ZLI in *Pax6*$^{-/-}$ mutants (Figures 2B and 6V–6X). These findings indicate that altered patterns of *Ngn2*, Ascl1, and *Nkx2.2* expression around the thalamic/prethalamic border of *Pax6*$^{-/-}$ mutants are dependent on Shh signaling. Our finding that the normal expression of these three genes is not Shh dependent indicates that other factors can maintain their normal patterns. They suggest that enhanced Shh signaling is a major contributor to many diencephalic patterning defects in *Pax6*$^{-/-}$ mutants.

We examined the potential functional consequence of the slight increase in Shh signaling in the *Pax6*$^{-/-}$ cortex but could not detect any effects of even high doses of vismodegib on the abnormal patterning in this region. For example, loss of Pax6 causes upregulation of Ascl1 expression in the cortex (Figures S6E and S6F), but vismodegib did not reverse this defect (Figure S6G). This indicates that the small upregulation of *Shh* expression in *Pax6*$^{-/-}$ cortex is not a significant cause of patterning defects in this region, highlighting regional differences in Pax6's mode of action.

Evidence that Pax6 Might Directly Regulate the Shh Promoter

We carried out luciferase assays using a 775 bp sequence corresponding to the *Shh* promoter (Table S1; Mutoh et al., 2010) (Figure 7A). Inclusion of the *Shh* promoter into the firefly luciferase reporter construct caused a large increase in firefly luciferase over Renilla luciferase activity; this increase was significantly reduced when cells were co-transfected with a Pax6-expressing construct (Mi et al., 2013). Chromatin immunoprecipitation (ChIP) experiments (Figure 7B) showed significant enrichment of fragments containing *Shh* promoter sequence (Table S1) compared to that of fragments containing *Syt8* promoter (a Pax6 nonbound control; Mi et al., 2013), demonstrating that Pax6 binds to the *Shh* promoter in vivo. Interestingly, bioinformatics using position weight matrices based on previously reported Pax6 binding sites did not identify the likely positions of Pax6 binding within the *Shh* promoter, indicating that Pax6 binds this region through one or more previously unrecognized, noncanonical sites.

We also tested whether an indirect mechanism might contribute to the upregulation of *Shh* in *Pax6*$^{-/-}$ diencephalic cells. It was possible that Pax6 loss might increase Wnt signaling around the ZLI, and this might cause upregulation of *Shh* because early Wnt expression in the ZLI permits the induction of *Shh* (Martinez-Ferre et al., 2013). We used a β-galactosidase transgenic reporter (BAT-gal) (Maretto et al., 2003) to show strong Wnt/β-catenin signaling around the ZLI whose domain expands in *Pax6*$^{-/-}$ mutants (Figures S7A–S7F). In chimeras, however, we found no evidence that clusters of *Pax6*$^{-/-}$ cells expressed increased levels of *Axin2* and *Lef1* (Figures S7G–S7L), which are readouts of levels of Wnt signaling (Hsu et al., 1998; Jho et al., 2002), indicating that increased Wnt signaling is unlikely to be a cause of changes in *Shh* expression by *Pax6*$^{-/-}$ diencephalic cells.

DISCUSSION

Previous studies showed that loss of Pax6 results in diencephalic patterning defects including expansion of the ZLI (Grindley et al., 1997; Pratt et al., 2000; Chatterjee et al., 2014), but

the mechanisms were unclear. We find that a combination of cell-autonomous and non-cell-autonomous effects is responsible. Pax6 is required cell autonomously to repress diencephalic *Shh* expression. Some of the major patterning defects that occur around the ZLI when Pax6 is absent are caused by enhanced Shh activity. We show that expansion of the ZLI and territories around the thalamic/prethalamic border is caused by cells acquiring abnormal molecular identities. Our main findings are summarized in Figures 7C–7E.

Theoretical studies by others have indicated that the involvement in control systems of elements that mutually repress each other, such as *Shh* and *Pax6*, can enhance the system's robustness by buffering it against stochastic, interindividual fluctuations or temporal changes in morphogen levels and can generate bistability (Sokolowski et al., 2012). These properties are exactly those required within the diencephalon, which is a relatively small but intricately patterned structure, to maintain its cells in either a ZLI or a non-ZLI state with a sharp, reproducibly positioned transition between them. We propose that direct repression of *Shh* by Pax6 creates a feedback loop that is critical for the precision of normal diencephalic patterning by ensuring extremely tight, robust control of the size and influence of the ZLI.

Several aspects of our findings highlight the importance of the context within which interactions between regulatory molecules occur for their outcomes. Although previous studies have shown that Shh can repress *Pax6* expression, including at the ZLI (Ericson et al., 1997; Kiecker and Lumsden, 2004; Macdonald et al., 1995), our results show that this does not always happen. We found no evidence for repression of the *Pax6* gene expression in diencephalic regions surrounding the normal position of the ZLI in $Pax6^{-/-}$ mutants. In these areas, expanded *Shh* expression caused an anticipated increase in the expression of its targets *Ptch1* and *Gli1*, but it did not prevent *Pax6* transcription, as shown by the abnormal double labeling of cells around the ZLI for both *Shh* and the *Pax6* reporter or *Pax6* mRNA. This suggests that, whereas Shh may normally contribute to the absence of Pax6 at the ZLI, elsewhere, the potential repressive effects of Shh on *Pax6* expression are likely moderated by other factors. Another example of context dependency is seen in the prethalamus, where Pax6 is required for Gsx2 expression, whereas in the telencephalon, loss of Pax6 results in upregulation of Gsx2 in cortex, where it would not normally be expressed (Rallu et al., 2002; Toresson et al., 2000; Yun et al., 2001). The way in which a transcription factor affects its target genes probably depends mainly on the nature of the cofactors that are available for it to interact with.

Another important aspect of our findings concerns the interaction between Shh and *Ptch1*. Many studies have shown that Shh can drive expression of *Ptch1* (Bai et al., 2002, 2004; Balaskas et al., 2012; Goodrich et al., 1996; Lee et al., 1997; Marigo and Tabin, 1996; Wijgerde et al., 2002). This explains the expression of *Ptch1* by cells adjacent to the ZLI in normal embryos and by $Pax6^{-/-}$ cells more widely throughout the diencephalon in mutants and chimeras, but it leaves unexplained the paradoxical observation that *Ptch1* is not expressed within the ZLI itself. *Ptch1* and *Gli1* are downregulated in regions expressing the highest levels of Shh not only at the ZLI but also along the neural tube (Marigo and Tabin, 1996), where cells become progressively refractory to Shh (Ribes et al., 2010), and in the expanded ZLI of $Pax6^{-/-}$ mutants. This suggests a biphasic response of *Ptch1* and *Gli1* to Shh, with very high levels of Shh repressing their expression (Figure 7C). Our findings using a Shh inhibitor suggest that this is indeed the case. They indicate that administration of Shh inhibitor to mutant embryos caused *Ptch1* upregulation at the expanded ZLI, where Shh levels were blocking *Ptch1* production, while simultaneously reducing *Ptch1* expression in cells outside the expanded ZLI, where lower levels of Shh were activating *Ptch1*.

In our model, Shh activates Dbx1 in the ZLI's ventricular zone and enhances Lhx5 expression in the overlying differentiating zone. Because the Shh receptor *Ptch1* is not expressed at the ZLI, it is likely that this activation and enhancement involve double repression, i.e., Ptch1 receptor activation likely represses *Dbx1* and *Lhx5*, and so loss of Ptch1 in the ventricular zone at the ZLI would allow expression of *Dbx1* by progenitors and Lhx5 by their progeny. Other factors must also be involved in fine-tuning the expression of *Dbx1* because *Dbx1* is not expressed throughout all of the Shh-rich ZLI, but only in its rostral part. Lineage analysis has shown that progeny from the ZLI are incorporated into the rostral vLG, a nucleus that comprises GABAergic neurons whose axons do not project to the cortex (Suzuki-Hirano et al., 2011; Vue et al., 2007, 2009). It is possible that there are subtle differences in the vLG neurons derived from the different types of ZLI progenitor.

In summary, we found that mutual antagonism between *Pax6* and *Shh*, involving cell-autonomous repression of *Shh* by Pax6, constrains the development of the ZLI, its production of Shh, and its influence on surrounding diencephalon. Pax6 is likely to have similar effects on *Shh* in other regions of the CNS, including the cortex (present findings and Mi et al., 2013) and the spinal cord, where its misexpression has been shown to reduce *Shh* expression (Lek et al., 2010). The functional importance of this repression outside the diencephalon is currently unclear; we show here that inhibition of Shh signaling in $Pax6^{-/-}$ cortex does not prevent abnormal cortical patterning. In the diencephalon, however, we conclude that Pax6 plays many of its essential roles in patterning by cell autonomously regulating Shh expression at the ZLI.

EXPERIMENTAL PROCEDURES

Animals

Animals were bred in-house following Home Office (UK) regulations. The *Pax6* null allele used was $Pax6^{SeyEd}$. Pax6-reporter mice were DTy54 (Tyas et al., 2006). *Gsx2cre* mice were from Kessaris et al. (2006), and $Ngn2cre^{ER}$ mice were from Zirlinger et al. (2002). *BAT-gal* transgenic mice are described in Maretto et al. (2003).

Chimera Production

$Pax6^{-/-}$ and wild-type embryonic stem (ES) cells were stably transfected with tau-GFP expression construct pTP6 (Pratt et al., 2000). Chimeric embryos were produced by injection of $Pax6^{-/-}$ tau-GFP or $Pax6^{+/+}$ tau-GFP ES cells into blastocysts.

Immunofluorescence

Antibodies used were mouse anti-Islet1 (39.4D5), mouse anti-Lhx1/Lhx5 (4F2), and mouse anti-Nkx2.2 (74.5A5) obtained from the Developmental Studies

Hybridoma Bank (University of Iowa), mouse anti-Ascl1 (BD Biosciences), mouse anti-Ngn2 (clone 7G4; Lo et al., 2002), rabbit anti-Olig3 (Chemicon), rabbit anti-Sox2 (Ab5603; Chemicon), goat and rabbit anti-GFP (Abcam), and mouse anti-GFP (Roche).

In Situ Hybridization

Probes were labeled with digoxigenin, fluorescein, or dinitrophenol (DNP). For fluorescence double in situ hybridization, the probes were detected sequentially, and the slides were incubated in 10 mM HCl before detection of the second probe.

Vismodegib Treatment

We administrated GDC-0449 (Selleckchem) at different concentrations by oral gavage at E9.5. Suspensions of GDC-0449 powder were prepared in methylcellulose-Tween vehicle (MCT) (Lipinski et al., 2010). Controls were given MCT vehicle.

Quantitative ChIP

DNA-protein complexes were precipitated with anti-Pax6 antibody (Covance) or with anti-immunoglobulin G (IgG) antibody (Abcam) (Sansom et al., 2009). Primer pairs for quantitative PCR (qPCR) are given in Table S1. The amount of qPCR product obtained with anti-Pax6 antibody was expressed relative to that obtained with anti-IgG antibody.

Luciferase Assays

Shh promoter sequence (Table S1) was cloned into pGLA4.10 promoterless firefly luciferase reporter vector (Promega). Pax6 was expressed using the pCMV-Pax6 construct (Mi et al., 2013). The Renilla luciferase vector was pRLSV40 (Promega). Human embryonic kidney 293 cells were transfected using Lipofectamine 2000 (Invitrogen), harvested 48 hr after transfection, and analyzed with the Dual-Luciferase Reporter Assay System using the GloMax luminometer (both Promega).

SUPPLEMENTAL INFORMATION

Supplemental Information includes seven figures and one table and can be found with this article online at http://dx.doi.org/10.1016/j.celrep.2014.07.051.

AUTHOR CONTRIBUTIONS

I.M.C. and M.N.M. did most of the experiments in collaboration with M.M. and helped write the manuscript. I.Q.-U. did experiments with vismodegib. D.M. did ChIP assays. T.S. contributed data on null mutants. D.J.P. conceived and supervised the work and wrote the manuscript.

ACKNOWLEDGMENTS

We thank Trudi Gillespie (IMPACT Facility) for help with imaging and Vicky Brewis for contributing to some experiments. Funding was from the MRC, UK (J003662/1 and G0800429), and the Wellcome Trust, UK (08420).

Received: July 31, 2013
Revised: June 24, 2014
Accepted: July 27, 2014
Published: August 28, 2014

REFERENCES

Bai, C.B., Auerbach, W., Lee, J.S., Stephen, D., and Joyner, A.L. (2002). Gli2, but not Gli1, is required for initial Shh signaling and ectopic activation of the Shh pathway. Development *129*, 4753–4761.

Bai, C.B., Stephen, D., and Joyner, A.L. (2004). All mouse ventral spinal cord patterning by hedgehog is Gli dependent and involves an activator function of Gli3. Dev. Cell *6*, 103–115.

Balaskas, N., Ribeiro, A., Panovska, J., Dessaud, E., Sasai, N., Page, K.M., Briscoe, J., and Ribes, V. (2012). Gene regulatory logic for reading the Sonic Hedgehog signaling gradient in the vertebrate neural tube. Cell *148*, 273–284.

Chatterjee, M., Guo, Q., Weber, S., Scholpp, S., and Li, J.Y. (2014). Pax6 regulates the formation of the habenular nuclei by controlling the temporospatial expression of Shh in the diencephalon in vertebrates. BMC Biol. *12*, 13.

Ericson, J., Rashbass, P., Schedl, A., Brenner-Morton, S., Kawakami, A., van Heyningen, V., Jessell, T.M., and Briscoe, J. (1997). Pax6 controls progenitor cell identity and neuronal fate in response to graded Shh signaling. Cell *90*, 169–180.

Gajović, S., St-Onge, L., Yokota, Y., and Gruss, P. (1997). Retinoic acid mediates Pax6 expression during in vitro differentiation of embryonic stem cells. Differentiation *62*, 187–192.

Goodrich, L.V., Johnson, R.L., Milenkovic, L., McMahon, J.A., and Scott, M.P. (1996). Conservation of the hedgehog/patched signaling pathway from flies to mice: induction of a mouse patched gene by Hedgehog. Genes Dev. *10*, 301–312.

Grindley, J.C., Hargett, L.K., Hill, R.E., Ross, A., and Hogan, B.L. (1997). Disruption of PAX6 function in mice homozygous for the Pax6Sey-1Neu mutation produces abnormalities in the early development and regionalization of the diencephalon. Mech. Dev. *64*, 111–126.

Hashimoto-Torii, K., Motoyama, J., Hui, C.C., Kuroiwa, A., Nakafuku, M., and Shimamura, K. (2003). Differential activities of Sonic hedgehog mediated by Gli transcription factors define distinct neuronal subtypes in the dorsal thalamus. Mech. Dev. *120*, 1097–1111.

Hirata, T., Nakazawa, M., Muraoka, O., Nakayama, R., Suda, Y., and Hibi, M. (2006). Zinc-finger genes Fez and Fez-like function in the establishment of diencephalon subdivisions. Development *133*, 3993–4004.

Hsu, S.C., Galceran, J., and Grosschedl, R. (1998). Modulation of transcriptional regulation by LEF-1 in response to Wnt-1 signaling and association with beta-catenin. Mol. Cell. Biol. *18*, 4807–4818.

Inamura, N., Ono, K., Takebayashi, H., Zalc, B., and Ikenaka, K. (2011). Olig2 lineage cells generate GABAergic neurons in the prethalamic nuclei, including the zona incerta, ventral lateral geniculate nucleus and reticular thalamic nucleus. Dev. Neurosci. *33*, 118–129.

Jeong, J.Y., Einhorn, Z., Mathur, P., Chen, L., Lee, S., Kawakami, K., and Guo, S. (2007). Patterning the zebrafish diencephalon by the conserved zinc-finger protein Fezl. Development *134*, 127–136.

Jeong, Y., Dolson, D.K., Waclaw, R.R., Matise, M.P., Sussel, L., Campbell, K., Kaestner, K.H., and Epstein, D.J. (2011). Spatial and temporal requirements for sonic hedgehog in the regulation of thalamic interneuron identity. Development *138*, 531–541.

Jho, E.H., Zhang, T., Domon, C., Joo, C.K., Freund, J.N., and Costantini, F. (2002). Wnt/beta-catenin/Tcf signaling induces the transcription of Axin2, a negative regulator of the signaling pathway. Mol. Cell. Biol. *22*, 1172–1183.

Kessaris, N., Fogarty, M., Iannarelli, P., Grist, M., Wegner, M., and Richardson, W.D. (2006). Competing waves of oligodendrocytes in the forebrain and postnatal elimination of an embryonic lineage. Nat. Neurosci. *9*, 173–179.

Kiecker, C., and Lumsden, A. (2004). Hedgehog signaling from the ZLI regulates diencephalic regional identity. Nat. Neurosci. *7*, 1242–1249.

Kitamura, K., Miura, H., Yanazawa, M., Miyashita, T., and Kato, K. (1997). Expression patterns of Brx1 (Rieg gene), Sonic hedgehog, Nkx2.2, Dlx1 and Arx during zona limitans intrathalamica and embryonic ventral lateral geniculate nuclear formation. Mech. Dev. *67*, 83–96.

Lee, J., Platt, K.A., Censullo, P., and Ruiz i Altaba, A. (1997). Gli1 is a target of Sonic hedgehog that induces ventral neural tube development. Development *124*, 2537–2552.

Lek, M., Dias, J.M., Marklund, U., Uhde, C.W., Kurdija, S., Lei, Q., Sussel, L., Rubenstein, J.L., Matise, M.P., Arnold, H.H., et al. (2010). A homeodomain feedback circuit underlies step-function interpretation of a Shh morphogen gradient during ventral neural patterning. Development *137*, 4051–4060.

Lipinski, R.J., Song, C., Sulik, K.K., Everson, J.L., Gipp, J.J., Yan, D., Bushman, W., and Rowland, I.J. (2010). Cleft lip and palate results from

Hedgehog signaling antagonism in the mouse: phenotypic characterization and clinical implications. Birth Defects Res. A Clin. Mol. Teratol. *88*, 232–240.

Lo, L., Dormand, E., Greenwood, A., and Anderson, D.J. (2002). Comparison of the generic neuronal differentiation and neuron subtype specification functions of mammalian achaete-scute and atonal homologs in cultured neural progenitor cells. Development *129*, 1553–1567.

Macdonald, R., Barth, K.A., Xu, Q., Holder, N., Mikkola, I., and Wilson, S.W. (1995). Midline signalling is required for Pax gene regulation and patterning of the eyes. Development *121*, 3267–3278.

Maretto, S., Cordenonsi, M., Dupont, S., Braghetta, P., Broccoli, V., Hassan, A.B., Volpin, D., Bressan, G.M., and Piccolo, S. (2003). Mapping Wnt/beta-catenin signaling during mouse development and in colorectal tumors. Proc. Natl. Acad. Sci. USA *100*, 3299–3304.

Marigo, V., and Tabin, C.J. (1996). Regulation of patched by sonic hedgehog in the developing neural tube. Proc. Natl. Acad. Sci. USA *93*, 9346–9351.

Martinez-Ferre, A., Navarro-Garberi, M., Bueno, C., and Martinez, S. (2013). Wnt signal specifies the intrathalamic limit and its organizer properties by regulating Shh induction in the alar plate. J. Neurosci. *33*, 3967–3980.

Mastick, G.S., Davis, N.M., Andrew, G.L., and Easter, S.S., Jr. (1997). Pax-6 functions in boundary formation and axon guidance in the embryonic mouse forebrain. Development *124*, 1985–1997.

Mi, D., Carr, C.B., Georgala, P.A., Huang, Y.T., Manuel, M.N., Jeanes, E., Niisato, E., Sansom, S.N., Livesey, F.J., Theil, T., et al. (2013). Pax6 exerts regional control of cortical progenitor proliferation via direct repression of Cdk6 and hypophosphorylation of pRb. Neuron *78*, 269–284.

Miyoshi, G., Hjerling-Leffler, J., Karayannis, T., Sousa, V.H., Butt, S.J., Battiste, J., Johnson, J.E., Machold, R.P., and Fishell, G. (2010). Genetic fate mapping reveals that the caudal ganglionic eminence produces a large and diverse population of superficial cortical interneurons. J. Neurosci. *30*, 1582–1594.

Mutoh, H., Hayakawa, H., Sashikawa, M., Sakamoto, H., and Sugano, K. (2010). Direct repression of Sonic Hedgehog expression in the stomach by Cdx2 leads to intestinal transformation. Biochem. J. *427*, 423–434.

Pratt, T., Vitalis, T., Warren, N., Edgar, J.M., Mason, J.O., and Price, D.J. (2000). A role for Pax6 in the normal development of dorsal thalamus and its cortical connections. Development *127*, 5167–5178.

Pratt, T., Quinn, J.C., Simpson, T.I., West, J.D., Mason, J.O., and Price, D.J. (2002). Disruption of early events in thalamocortical tract formation in mice lacking the transcription factors Pax6 or Foxg1. J. Neurosci. *22*, 8523–8531.

Rallu, M., Corbin, J.G., and Fishell, G. (2002). Parsing the prosencephalon. Nat. Rev. Neurosci. *3*, 943–951.

Ribes, V., Balaskas, N., Sasai, N., Cruz, C., Dessaud, E., Cayuso, J., Tozer, S., Yang, L.L., Novitch, B., Marti, E., and Briscoe, J. (2010). Distinct Sonic Hedgehog signaling dynamics specify floor plate and ventral neuronal progenitors in the vertebrate neural tube. Genes. Dev *24*, 1186-200.

Robertshaw, E., Matsumoto, K., Lumsden, A., and Kiecker, C. (2013). Irx3 and Pax6 establish differential competence for Shh-mediated induction of GABAergic and glutamatergic neurons of the thalamus. Proc. Natl. Acad. Sci. USA *110*, E3919–E3926.

Rogers, K.W., and Schier, A.F. (2011). Morphogen gradients: from generation to interpretation. Annu. Rev. Cell Dev. Biol. *27*, 377–407.

Sansom, S.N., Griffiths, D.S., Faedo, A., Kleinjan, D.J., Ruan, Y., Smith, J., van Heyningen, V., Rubenstein, J.L., and Livesey, F.J. (2009). The level of the transcription factor Pax6 is essential for controlling the balance between neural stem cell self-renewal and neurogenesis. PLoS Genet. *5*, e1000511.

Scholpp, S., and Lumsden, A. (2010). Building a bridal chamber: development of the thalamus. Trends Neurosci. *33*, 373–380.

Scholpp, S., Wolf, O., Brand, M., and Lumsden, A. (2006). Hedgehog signalling from the zona limitans intrathalamica orchestrates patterning of the zebrafish diencephalon. Development *133*, 855–864.

Shimamura, K., Hartigan, D.J., Martinez, S., Puelles, L., and Rubenstein, J.L. (1995). Longitudinal organization of the anterior neural plate and neural tube. Development *121*, 3923–3933.

Sokolowski, T.R., Erdmann, T., and ten Wolde, P.R. (2012). Mutual repression enhances the steepness and precision of gene expression boundaries. PLoS Comput. Biol. *8*, e1002654.

Suzuki-Hirano, A., Ogawa, M., Kataoka, A., Yoshida, A.C., Itoh, D., Ueno, M., Blackshaw, S., and Shimogori, T. (2011). Dynamic spatiotemporal gene expression in embryonic mouse thalamus. J. Comp. Neurol. *519*, 528–543.

Taipale, J., Cooper, M.K., Maiti, T., and Beachy, P.A. (2002). Patched acts catalytically to suppress the activity of Smoothened. Nature *418*, 892–897.

Toresson, H., Potter, S.S., and Campbell, K. (2000). Genetic control of dorsal-ventral identity in the telencephalon: opposing roles for Pax6 and Gsh2. Development *127*, 4361–4371.

Tyas, D.A., Simpson, T.I., Carr, C.B., Kleinjan, D.A., van Heyningen, V., Mason, J.O., and Price, D.J. (2006). Functional conservation of Pax6 regulatory elements in humans and mice demonstrated with a novel transgenic reporter mouse. BMC Dev. Biol. *6*, 21.

Vue, T.Y., Aaker, J., Taniguchi, A., Kazemzadeh, C., Skidmore, J.M., Martin, D.M., Martin, J.F., Treier, M., and Nakagawa, Y. (2007). Characterization of progenitor domains in the developing mouse thalamus. J. Comp. Neurol. *505*, 73–91.

Vue, T.Y., Bluske, K., Alishahi, A., Yang, L.L., Koyano-Nakagawa, N., Novitch, B., and Nakagawa, Y. (2009). Sonic hedgehog signaling controls thalamic progenitor identity and nuclei specification in mice. J. Neurosci. *29*, 4484–4497.

Warren, N., and Price, D.J. (1997). Roles of Pax-6 in murine diencephalic development. Development *124*, 1573–1582.

Wijgerde, M., McMahon, J.A., Rule, M., and McMahon, A.P. (2002). A direct requirement for Hedgehog signaling for normal specification of all ventral progenitor domains in the presumptive mammalian spinal cord. Genes Dev. *16*, 2849–2864.

Yun, K., Potter, S., and Rubenstein, J.L. (2001). Gsh2 and Pax6 play complementary roles in dorsoventral patterning of the mammalian telencephalon. Development *128*, 193–205.

Zhou, C.J., Pinson, K.I., and Pleasure, S.J. (2004). Severe defects in dorsal thalamic development in low-density lipoprotein receptor-related protein-6 mutants. J. Neurosci. *24*, 7632–7639.

Zirlinger, M., Lo, L., McMahon, J., McMahon, A.P., and Anderson, D.J. (2002). Transient expression of the bHLH factor neurogenin-2 marks a subpopulation of neural crest cells biased for a sensory but not a neuronal fate. Proc. Natl. Acad. Sci. USA *99*, 8084–8089.